Numerical Solution of Hydrodynamic Electrically Conducting Fluid Flow over a Stretching Sheet

Padmini Kaji[1], Jagadish V. Tawade [2](§), Mahadev M. Baradar[3], Pradeep G. Janthe[4]
[1]Research Scholar, Bheemanna Khandre Institute of Technology, Bhalki-585328, Karnataka, INDIA
e-mail: [1]pskaji123@gmail.com
[2, 4]Department of Mathematics, Vishwakarma University Pune, INDIA.
e-mail: [2]jagadish.tawade@vupune.ac.in(§), [4]pradeepjanthe@gmail.com
[3]Basaveshwar Engineering College (Autonomous), Bagalkot-587103, INDIA
e-mail: [3]mmbbec@gmail.com
§-**Corresponding Author:** Jagadish V. Tawade

Article Info
Page Number:12714 - 12730
Publication Issue:
Vol 71 No. 4 (2022)

Article History
Article Received*: 15 September 2022*
Revised: *24 October 2022*
Accepted: *18 November 2022*
Publication: *21 December 2022*

Abstract: This study looks at the numerical results of magneto hydrodynamic liquid flowing across a stretching sheet at its stagnation point while also experiencing chemical reaction, viscous dissipation, thermal radiation and variable magnetic field. The fundamental partial differential equations that regulate physical phenomena are converted into non-linear ordinary differential equations by using the appropriate similarity transformations. Later, resolved by numerically using the Mathematica. Results of the effect of the non-dimensional parameters like Velocity ratio parameter (λ), Porosity (k), Magnetic parameter (M), Radiation parameter (R), Chemical reaction parameter (γ) etc. on velocity, concentration, and the temperature profiles for their various values were analysed and presented graphically. The numerical evaluation of the physical quantities was provided in tabular form for the various values of the relevant stream parameters.

Keywords: Magnetohydrodynamics, Chemical reaction, Velocity ratio parameter, Boundary layer flow, Stretching Sheet.

1. Introduction

The research on boundary layer flow Due to their wide range of applications in research and industry, together with heat transfer over the linearly stretched plate, they have seen some success in recent years. The boundary layer flow and heat transfer of an electrically conducting viscous fluid over a stretching sheet are the subjects of the study, studied by L. J. Crane in 1970 [1].

P. Carragher; et. al. studied the investigation of the heat transfers from a stretching sheet that emerges from a slit and strikes a medium at rest; the sheet's speed is proportional to the distance from the slit; the temperature difference between the sheet and its surroundings is proportional to a power of the distance from the slit. For both medium and large Prandtl values, the heat transfer rate is determined [2]. The temperature distribution in a viscous, incompressible fluid flow generated by the stretching of a sheet that emerges through a slit in the stream is examined by B.K. Dutta et. al. [3].

On an exponentially stretched continuous surface with an exponential temperature distribution, the similarity solutions representing the steady plane (flow and thermal) boundary layers are investigated analytically and numerically by Magyari, E [4].

C. Ullmann investigated the Dynamic Light Scattering for Particle Size Determination by Microfiltration of Submicron-Sized and Nano-Sized Suspensions [5].

The American Society of Mechanical Engineers' winter annual meeting is where Choi first used the term "Nano fluid" in his important paper in 1995.

M. Ibrahim et. al. examined how a magnetic field affects a nanofluid's stagnation point flow and heat transfer to a stretching sheet. [6]. M. Subhas Abel et. al. has examined in his work that the study of effect of heat transfer an MHD flow within a boundary layer within Maxwell fluid over a stretching sheet [7].

Planar stagnation-point flow, also referred to as Hiemenz flow, was the subject of Schlichting's discussion in 1960. Particle deposition in this kind of system was studied by Chari and Rajagopalan. The study looks at the heat transfer and magnetohydrodynamics (MHD) stagnation point flow of a Williamson fluid in the direction of an exponentially stretched sheet buried in a thermally stratified medium exposed to suction studied by Ch.Vittal et. al. [8]. M. Subhas Abel et. al. studied the flow and heat transmission characteristics of a laminar liquid film over a flat, impermeable stretched sheet in the presence of a non-uniform heat source or sink have been studied using magneto hydrodynamic boundary layer analysis [9]. Amir Abbas recent study was to investigate the behaviour of heat transfer and magnetohydrodynamic Williamson nanofluid flow across a non-linear stretching sheet embedded in a porous media[10].

M. Subhas Abel et. al. analysed the study is conducted to determine how MHD and thermal radiation affect the two-dimensional steady flow of an upper-converted, incompressible Maxwell's fluid in the presence of an external magnetic field [11].

M. Tanyeri investigated the microfluidic integrated device for the precise control and containment of micro- and nanoscale particles in free solution. Single particles are caught in a stagnation point flow at the intersection of two intersecting microchannels using this device in his research [12].

The issue of stable laminar Nano fluid flow on a two-dimensional boundary layer using heat transfer of Cassona transverse the linearly extending sheet investigated by Jagadish V. Tawade et. al. in their recent research work [13].

The idea behind isolated microfluidic stagnation point flows, highlight several strategies for addressing them through experimentation, and then examine their applications in chemistry and the life sciences with a particular focus on micro-total-analysis systems which is illustrated by Ayoola T. Brimmo and Mohammad A. Qasaimeh [14].

Seth et. al studied the heat and mass diffusion of MHD stagnation point flow of electromagnetic nanofluid with the Joule heating and viscous dissipation in the presence of convective and thermal radiation [15]. The movement of a nanofluid toward a stretched surface from just a stagnation point. Further consideration is given to the consequences of thermophoresis and Brownian motion. The homotopy analysis method is used to develop the analytical solutions (HAM) report given by M. Mustafa et. al. [16]. Investigated is the unstable laminar flow of a micropolar incompressible fluid across a stretching sheet. Because of how the stretching velocity and surface temperature vary over time, the flow and temperature fields are unstable. Flow and heat transfer characteristics are thoroughly explored in relation to the effects of the unsteadiness parameter, material parameter, and Prandtl number[17]. G. S. Roopa et. al. used the model to study the impact of radiation on the heat transfer and flow of a dusty fluid over a stretched vertical surface during mixed convection boundary layers [18]. P. Besthapu et. al. examined the effects of velocity slip and heat radiation combined along a stretching surface with nonlinear convection. Also taken into account are MHD effects close to the Casson nanofluid's stagnation point flow [19]. N. N. Reddy et. al. their study focuses on the effects of viscous dissipation on free convection MHD flow through a porous media across an exponentially stretched surface when chemical reaction is present [20]. The unsteady tangent hyperbolic liquid stream scenario is where the flow computations with modified Hartmann numbers are placed it was investigated by S Abdal et. al. [21]. R. Mohana Ramana et. al. investigated In the presence of a chemical reaction, the effects of many slips and a heat source on the casson fluid's MHD stagnation point flow over a stretching sheet [22]. Alfunsa Prathiba examines the numerical outcome of magnetohydrodynamic liquid (MHD) flow across a stretchy sheet while chemical reaction and viscous dissipation are present [23].

The effects of magnetohydrodynamic flow within a Jeffery fluid's boundary layer in a porous material across a contracting/expanding sheet are discussed by Shaila S. Benal et. al. [24]. C. N. Guled et. al. Studied on an isothermal porous streach surface, laminar magneto hydrodynamic flow (MHD flow) on the upper-convected Maxwell fluid has been studied using the optimal homotopy analysis technique (OHAM) [25].

Numerous researchers have concentrated their research on the stagnation point flow of nanofluids across a stretching surface as a result of the vast range of applications of nanofluids in various technologies and sectors. This paper aims to consider the effects of radiation and stagnation point flow in an MHD flow against a linearly stretching surface with variable surface thickness along with heat and mass transfer characteristics were investigated. The paper is motivated by the aforementioned literature and applications. The boundary-layer approximation was used to formulate the problem. The effects of different flow-related variables on temperature and concentration zones were discussed and explored. Furthermore, numerical observations of the rates of heat, mass, and skin friction transmission were made.

2. Mathematical Formulation

Consider a two-dimensional laminar steady flow of an incompressible hydro magnetic viscous, electrically conducting flow over a stretching sheet. The system's starting point is the slit from which the sheet is drawn. In this coordinate the frame of the axis is taken along the path of the continuous stretching plane.

Considering the stretching sheet's velocity to be $U_w(x) = bx$ and the free stream flow's velocity to be $U_\infty(x) = ax$, where a, b are positive constants and x is the coordinate all along the stretching plane.

The flow is carried out at ≥ 0 , where y is the perpendicular to the stretching sheet coordinate. Let T_w, C_w be the temperature and concentration of the Nano-fluid at the stretching layer and let $T_\infty and\ C_\infty$ be the ambient temperature and concentration.

$$\frac{\partial u}{\partial x}+\frac{\partial v}{\partial y}=0 \quad (1)$$

$$u\frac{\partial u}{\partial x}+v\frac{\partial u}{\partial y}=\nu\frac{\partial^2 u}{\partial y^2}+g\beta_t(T-T_\infty)+g\beta_c(C-C_\infty)-\frac{\nu}{k}u-\frac{\sigma {B_0}^2}{\rho}u+U_\infty\frac{\partial U_\infty}{\partial x} \quad (2)$$

$$u\frac{\partial T}{\partial x}+v\frac{\partial T}{\partial y}=\alpha\frac{\partial^2 T}{\partial y^2}-\frac{1}{\rho C_P}\frac{\partial q_r}{\partial y}+\frac{Q}{\rho C_P}(T-T_\infty)+\frac{\mu}{\rho C_P}\left(\frac{\partial u}{\partial y}\right)^2+\frac{\sigma {B_0}^2}{\rho C_P}u \quad (3)$$

$$u\frac{\partial C}{\partial x}+v\frac{\partial C}{\partial y}=D_B\frac{\partial^2 C}{\partial y^2}-K_r(C-C_\infty) \quad (4)$$

Where **u and v** are the elements of velocity along coordinate axes, T is the temperature, C is the concentration of species. The kinematic viscosity υ, ∝ is the thermal diffusivity, D_B is the Brownian motion coefficient [2], [20]. Make use of the Roseland [20] approximation for radiation, the radiative heat flux q_r is given by

$$q_r=\frac{-4\sigma^*}{3k^*}\frac{\partial T_1^4}{\partial y} \quad (5)$$

Where k* is the average absorption coefficient, σ* is the Stefan-Boltzmann constant. We presume that the temperature changes inside the flow sufficiently small. The expression T_1^4, enlarging in a Taylor series in powers of (T_1-T_∞) and ignoring higher-order terms we get $T_1^4 \approx 4T_\infty^3 T_1-3T_\infty^4$, hence [20],

$$q_r=\frac{-4\sigma^* T_\infty^3}{3k^*}\frac{\partial T}{\partial y} \quad \text{then,} \quad \frac{\partial q_r}{\partial y}=\frac{-16\sigma^* T_\infty^3}{3p c_p k^*}\frac{\partial^2 T}{\partial y^2} \quad (6)$$

The corresponding boundary conditions are

$$u_1=bx\,;\; v_1=0\,;\; T_1=T_w\,;\; C_1=C_w \quad at\; y=0$$
$$u_1=U_\infty=ax\,, T_1=T_\infty\,;\; C_1=C_\infty \quad as\; y\to\infty \quad (7)$$

Introducing the similarity transformations, which satisfy the equation of continuity

$$u_1=\frac{\partial\psi}{\partial y} \quad and \quad v_1=-\frac{\partial\psi}{\partial x} \quad (8)$$

Such that

$$u_1=bxf'(\eta),v_1=-\sqrt{\nu b}f(\eta);\; \eta=\sqrt{\frac{b}{\nu}}y,\;\; \theta=\frac{T-T_\infty}{T_w-T_\infty},\;\; \emptyset=\frac{C-C_\infty}{C_w-C_\infty} \quad (9)$$

Substituting Equations (6), (8), (9) in equations (2)-(4) we get the following coupled nonlinear differential equations.

$$f'''+f\,f''+Gr\,\theta+Gm\,\phi-\left(M-1+\frac{1}{k}\right)(f')^2+\lambda^2=0 \quad (10)$$

$$\left(1+\frac{4}{3}R\right)\theta''+Pr[Ec\,[(f'')^2+M\,(f'-1)^2]+S\,\theta+f\,\theta']]=0 \quad (11)$$

$$\phi''+Sc\,[\,f\,\phi'-\gamma\phi\,]=0 \quad (12)$$

The parameters that are present in the above equations are, magnetic parameter M , Prandtl number P_r , Schmidt number S_c , Eckert number (Ec), chemical reaction rate parameter γ and the Source parameter S , R is the radiation parameter, λ is the velocity ratio parameter and 1/k Porosity parameter given as follows

$$P_r=\frac{\vartheta}{\alpha}, \quad M=\frac{\sigma B_0^2}{\rho b}, \frac{k_p^1}{\vartheta}=k\,, R=\frac{4\sigma^* T_\infty^3}{k^* k}, \lambda=\frac{a}{b},$$

$$E_c=\frac{b^2x^2}{(T-T_\infty)C_p}, S=\frac{Q}{\rho c_p b}, S_c=\frac{\vartheta}{D_B}, \gamma=\frac{k_r}{b}.$$

The transformed boundary conditions are

$$f(\eta)=0, f'(\eta)=1, \theta(\eta)=1, \phi(\eta)=1 \; as \; \to 0$$
$$f'(\eta)\to\lambda, \theta(\eta)\to 0, \emptyset(\eta)\to 0 \; as \; \eta\to\infty \qquad (13)$$

Where η is a similarity variable, f (η) is dimensionless stream velocity, θ (η) is a temperature profile, ∅(η) is a concentration and prime denotes the differentiation with respect to η. Physical Quantities are, C_f is the Local skin friction coefficient, the heat N_u and mass transfers Sh coefficients from the plate, respectively are given by

$$C_f=\frac{\tau_w}{\rho U_w^2} \Longrightarrow C_f\sqrt{Re}=f''(0)$$

$$N_u=\left(\frac{xq_w}{(T-T_\infty)}\right)_{y=0} \Longrightarrow \frac{N_u}{\sqrt{Re}}=-\theta'(0), Sh=\frac{-x\left(\frac{\partial c}{\partial y}\right)_{y=0}}{(C_w-C_\infty)} \Longrightarrow \frac{Sh}{\sqrt{Re}}=-\emptyset'(0)$$
(14)

Where $Re=\sqrt{\frac{bx^2}{\vartheta}}$ is the local Reynold's number.

3. Numerical Solution

The non-linear Ordinary Differential equations (10) -(12) along with the boundary conditions (13) are solved by using Mathematica, Runge-Kutta Fourth Order Shooting Techniques. For this, the aforementioned equations are transformed into the following first-order ODEs:

$$f(1)=f, f(2)=f', f(3)=f''; \; \theta(1)=\theta, \theta(2)=\theta'; \; \phi(1)=\phi, \phi(2)=\phi'$$

$$f'''=-f(1)f(2)+\left[M+\frac{1}{k}\right]f(2)-\lambda^2+[f(2)]^2$$

$$\theta''=\frac{-Pr}{\left[1+\frac{4R}{3}\right]}\left[Ec(f(3))^2+S\theta(1)+f(1)\theta(2)\right]$$

$$\phi''=Sc[\gamma\phi(1)-f(1)\phi(2)]$$

Along with the boundary conditions,

$$f(0)=0, f(2)=1, \theta(0)=1, \phi(0)=1$$
$$f(2)\to\lambda, \theta(1)\to 0, \phi(1)\to 0$$

4. Results And Discussion

The present results can be used in understanding more complex electrically conducting MHD fluid flow of heat and mass transfer over a stretching sheet embedded in a porous medium with viscous dissipation, thermal radiation and chemical reaction. A numerical study has been carried out to discuss the impacts of diverse parameters along with the local skin friction coefficient $-f''(0)$ and the local Nusselt number $-\theta'(0)$, The calculated values are presented in Figs. 2 to 18 and explained physically.

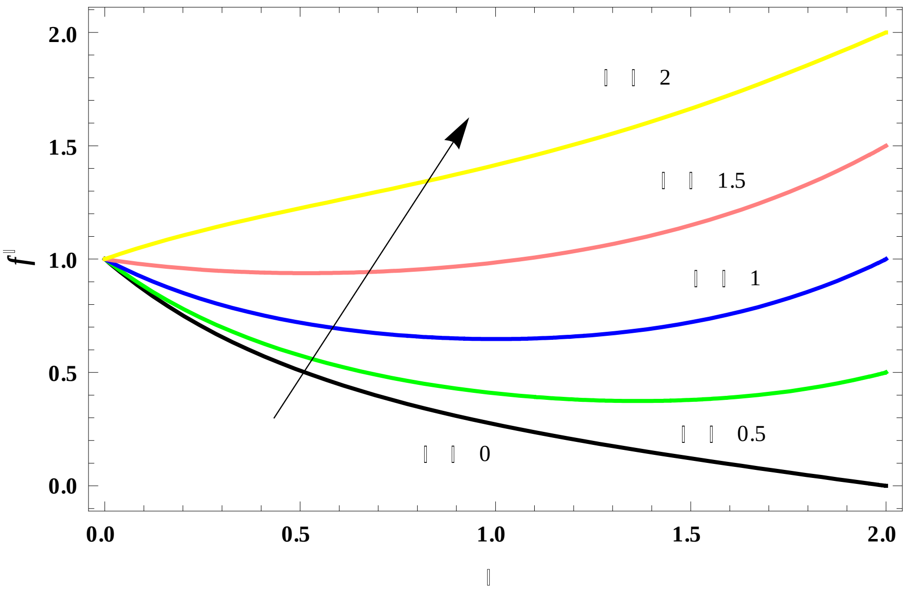

Figure 1: Impact of velocity ratio parameter (□□ on velocity

Figure.1. depicts the effects of velocity profile for various velocity ratio parameter values. From these figures it is evident that the free stream velocity is higher than stretched surface velocity, however, flow velocity increases and boundary layer thickness falls. (i e., λ >1).

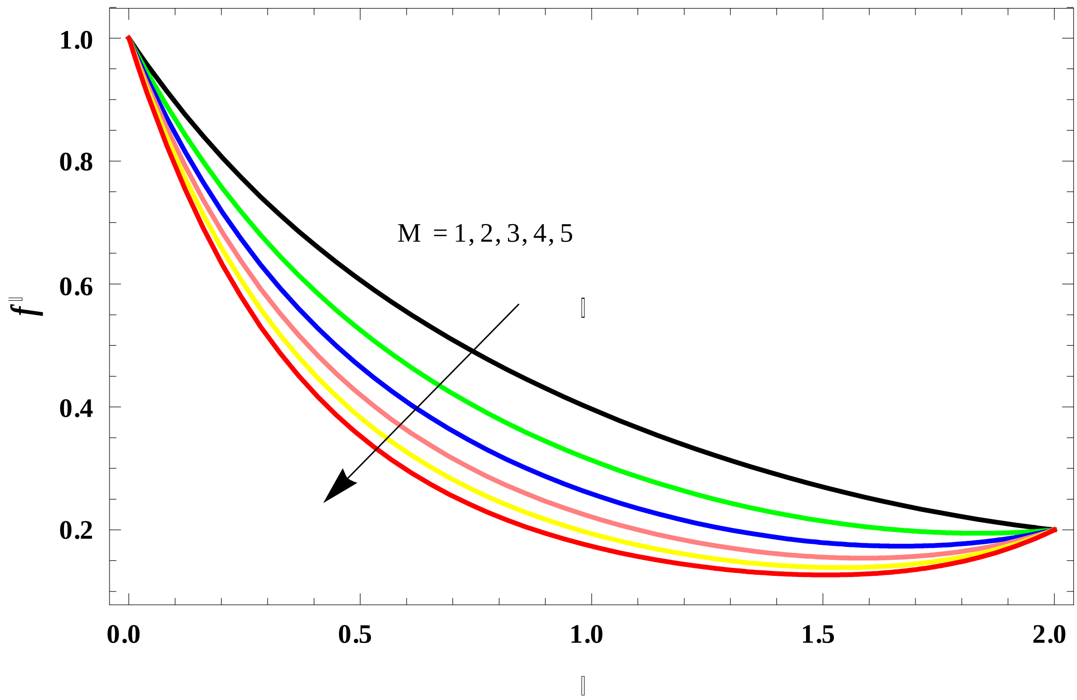

Figure 2: Impact of Magnetic parameter (M) on velocity

Figure.2. depicts the variations in the Velocity profile for different values of the Magnetic parameter (M). From the above figure it is seen that as the values of magnetic parameter increases, the velocity profile decreases in the boundary region.

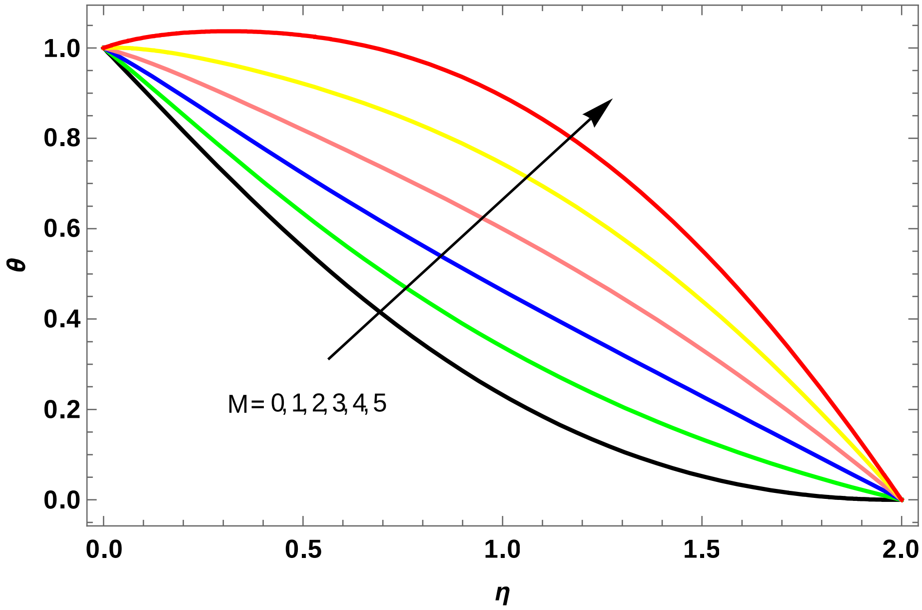

Figure 3: Impact of Magnetic parameter (M) on Temperature

Figure.3. Shows the effect of Temperature profile for different values of the Magnetic parameter (M). In the figure it is been observed that as magnetic parameter value increases the temperature profile increases.

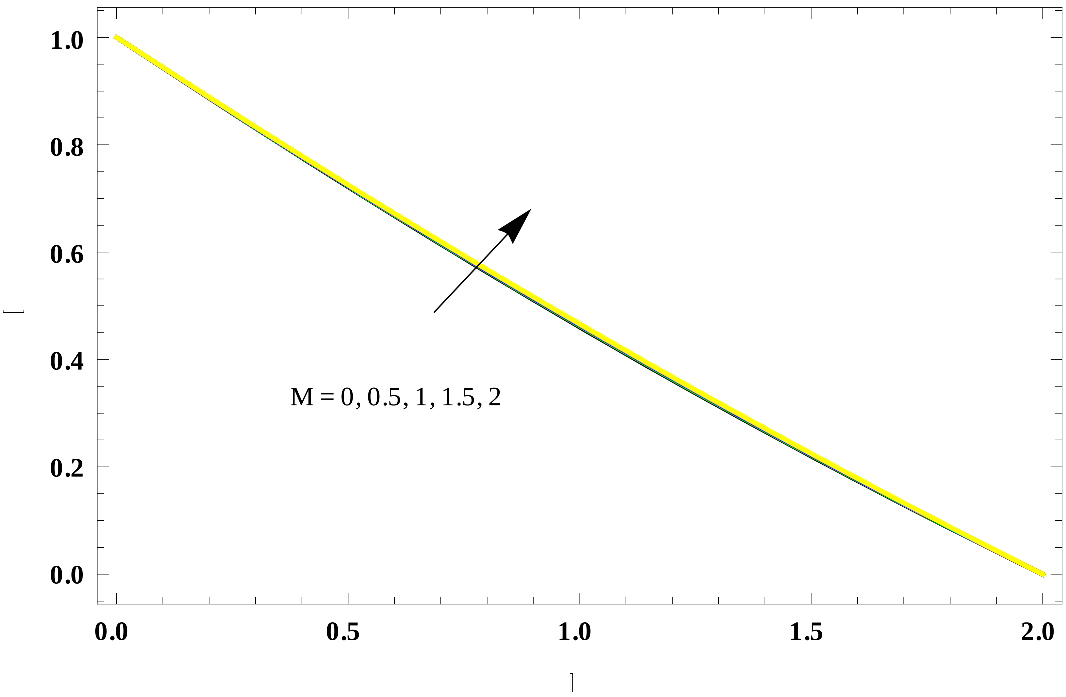

Figure 4: Impact of Magnetic parameter (M) on concentration

The increase in the value of Magnetic parameter decreases concentration profile as shown in Figure (4). As stated, increase of magnetic parameter diminishes the magnitude of velocity profiles in the boundary layer, this is because the applied transverse magnetic field produces a retarding Lorentz force and also for the enhancements in parameters such as the Radiation parameter (R), Eckert number (Ec), and Source parameter (S), Chemical reaction parameter (γ), the temperature distribution increases as shown in the Figure (5)-(8).

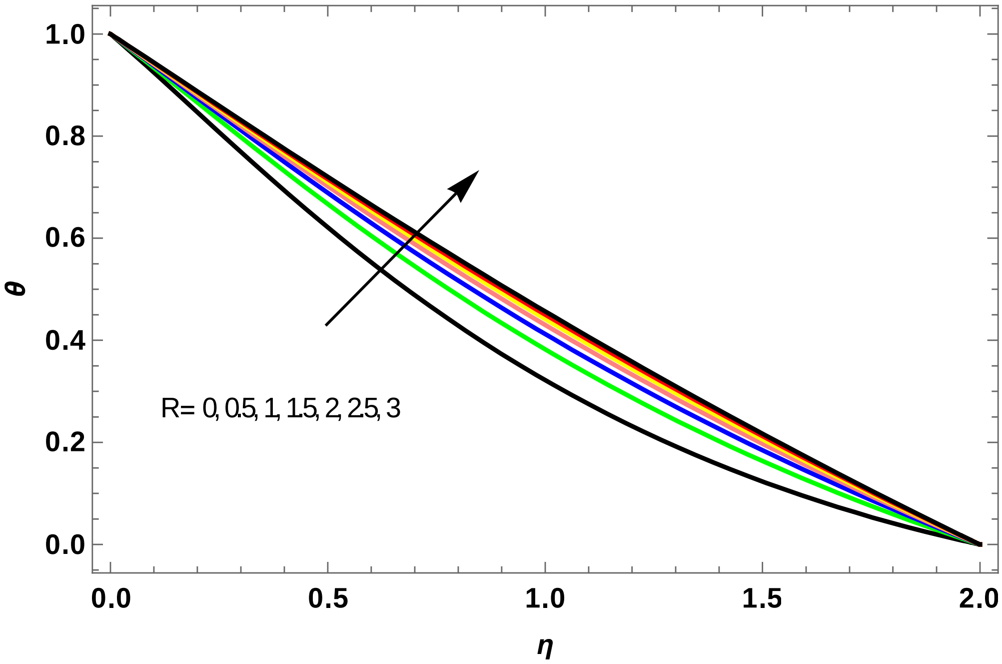

Figure 5: Impact of Radiation (R) on Temperature

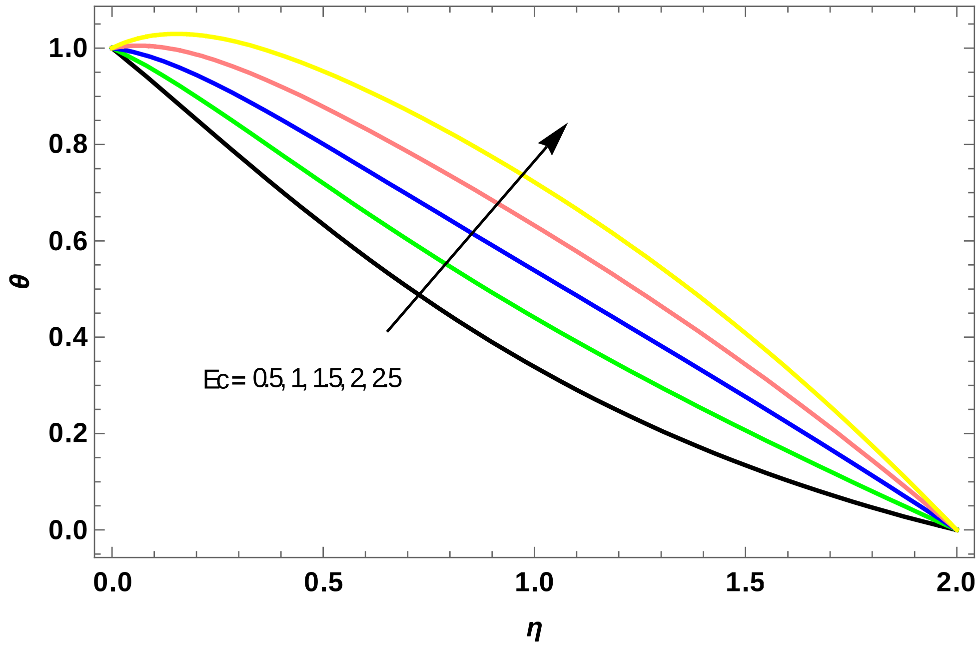

Figure. 6: Impact of Eckert number (Ec) on Temperature

In the above graph it is clearly seen that at the edge of the boundary when the values are 0.5, 1.0, 1.5 it is decreasing and similarly at 2.0, 2.5 it is increasing. An increase in the stretching rate of the sheet for higher values of Ec and thus a large enhancement through the motion of particles adjacent to the surface, which cause increment in the temperature in the fluid, particularly in the vicinity of the sheet.

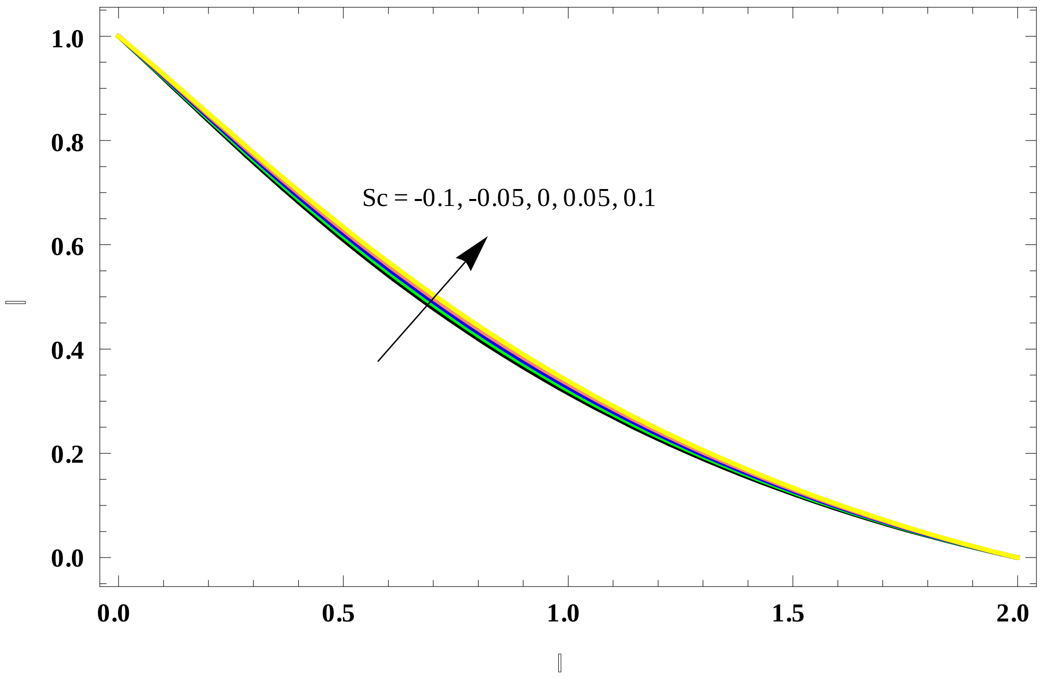

Figure. 7: Impact of source parameter (S) on temperature

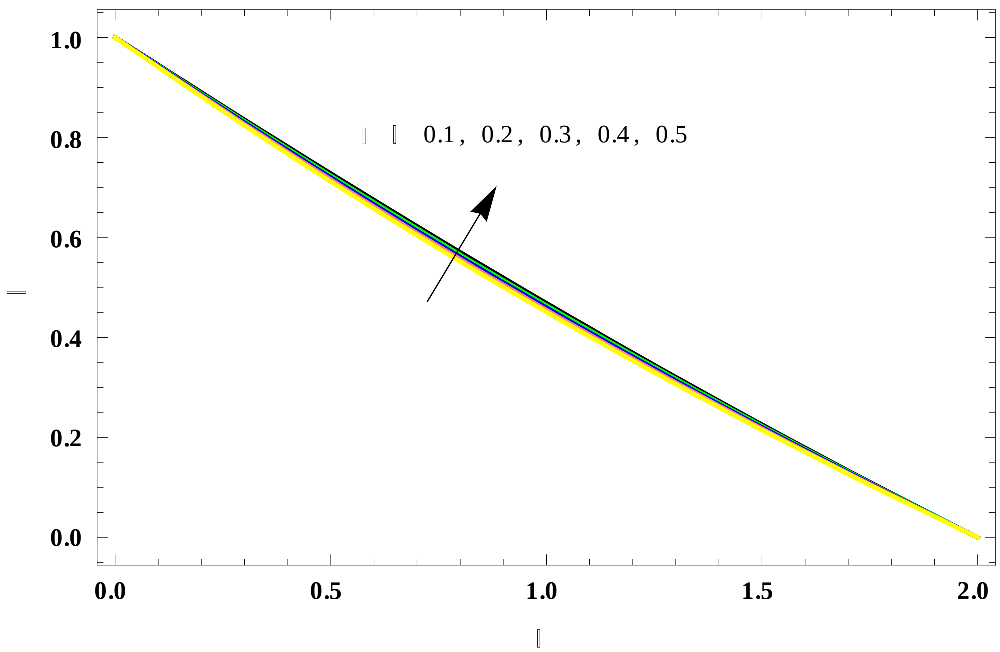

Figure 8: Impact of Chemical reaction parameter (γ) on concentration

The concentration profile slightly lowers while the Schmidt parameter Sc is raised. Because chemical molecular diffusivity decreases with increasing chemical reaction parameter values, the concentration boundary layer thickness decreases as the chemical reaction parameter is increased.

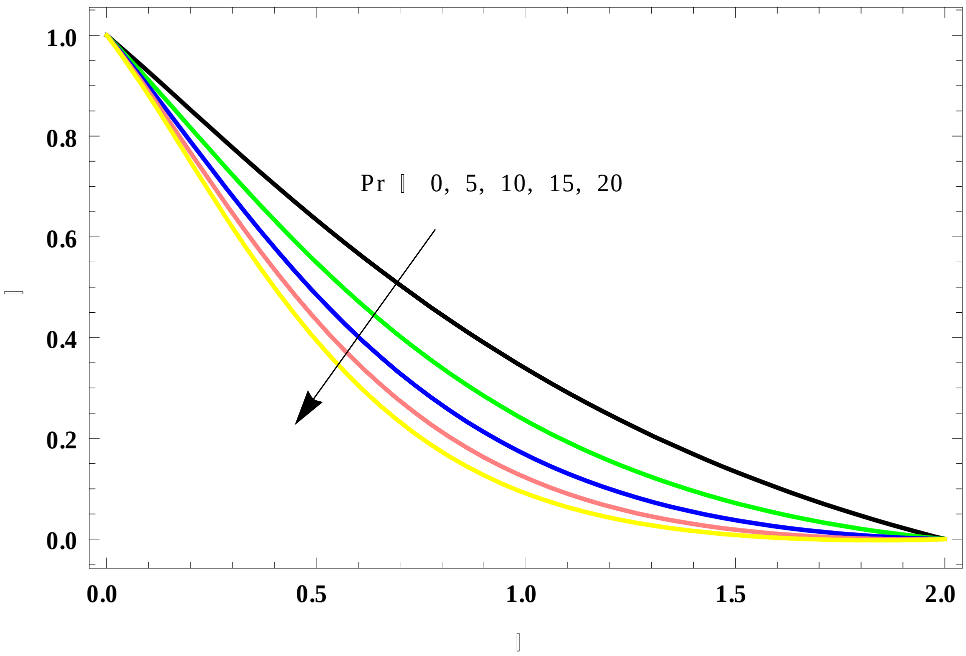

Figure. 9: Impact of Prandtl's number (Pr) on Temperature

Figure. 9. Shows the impact parameter of Prandtl number on temperature. The physical reason behind this phenomenon is that greater value of Pr relatively lower thermal conductivity and as consequence reduction in thermal boundary layer thickness and a decrement in the heat transfer rate over the boundary surface which causes to decrease temperature profile significantly.

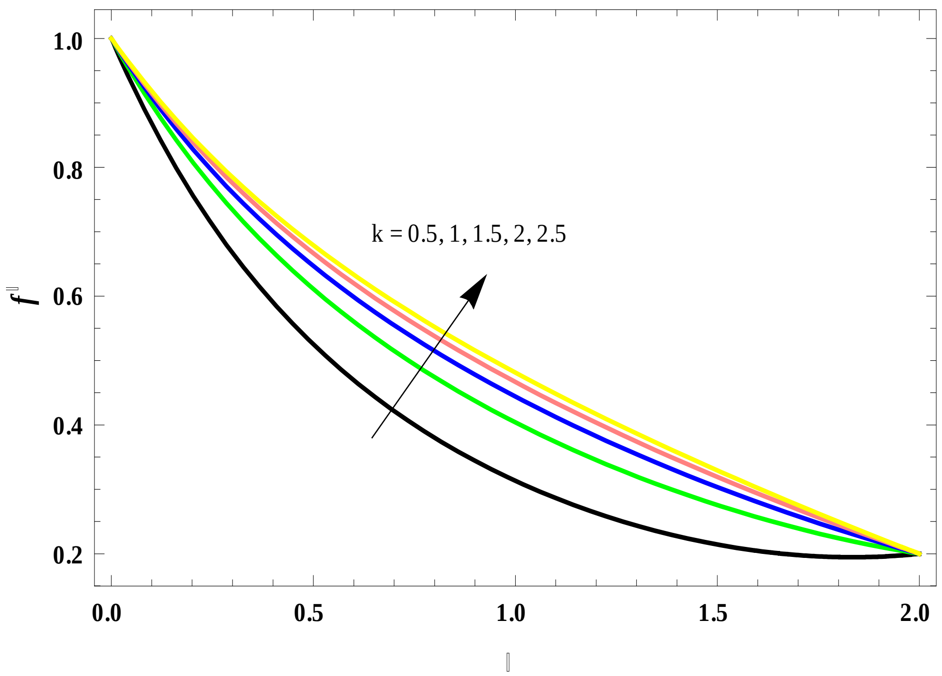

Figure 10 : Impact of Porous parameter (k) on Velocity y.

Figure 10. demonstrates how a porous parameter affects velocity. The porous parameter's value rises with velocity.

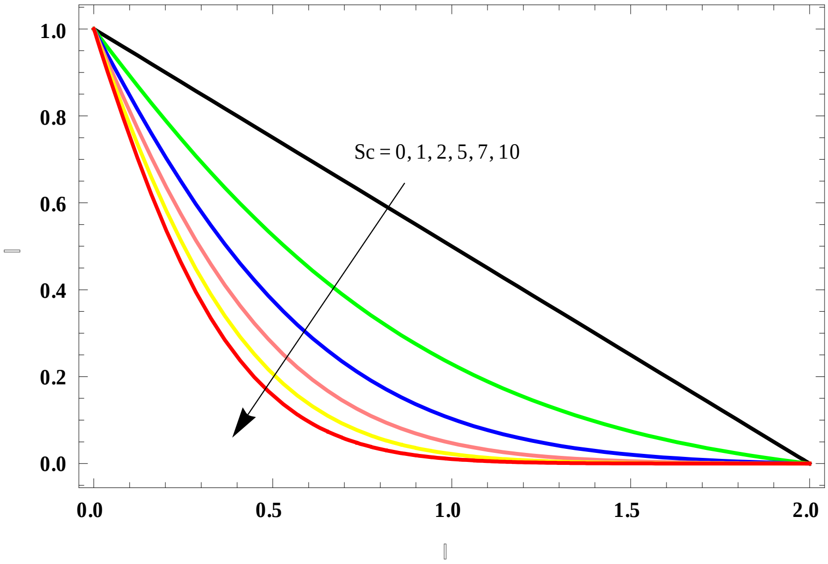

Figure 11: Impact of Schmidt number (Sc) on concentration profile

Figure 11. Shows the concentration profile becomes flatter as the Schmidt parameter Sc is raised. Because chemical molecular diffusivity decreases with increasing chemical reaction parameter values, the concentration boundary layer thickness decreases as the chemical reaction parameter is increased.

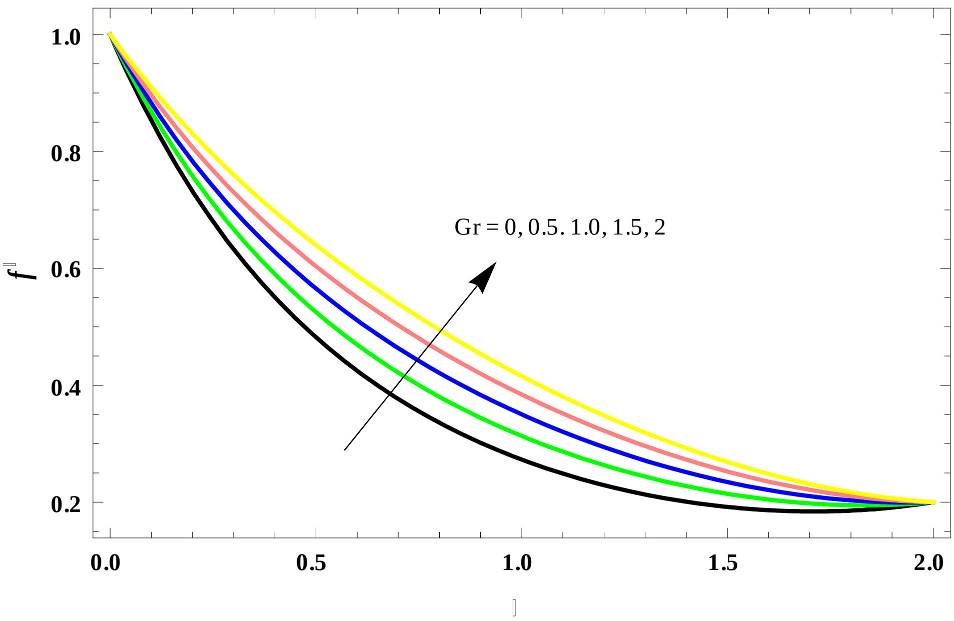

Figure 12: Impact of thermal Grashof number (Gr) on Velocity

Figure.12. Shows the variations in the Velocity profile for different values of the Grashof number(Gr). As the values of the Grashof number (Gr) increase, the velocity parameter decreases, as can be seen in the above figure.

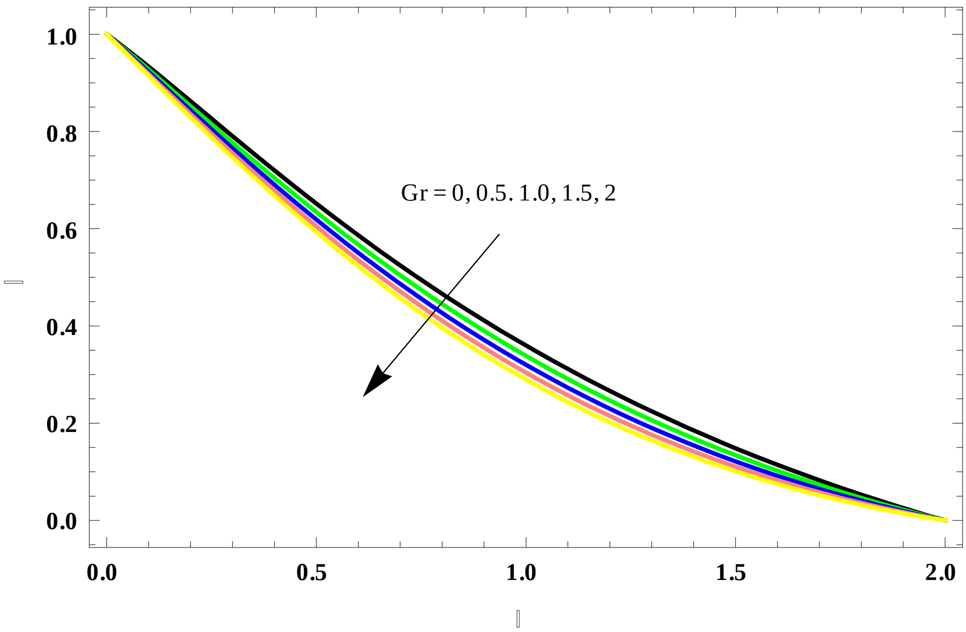

Figure 13: Impact of thermal Grashof number (Gr) on temperature profile

Figure 13. Shows the effect of temperature profile for different values of the Grashof number(Gr). In the figure it is observed that as the values of Grashof number(Gr) increases the temperature profile parameter decreases.

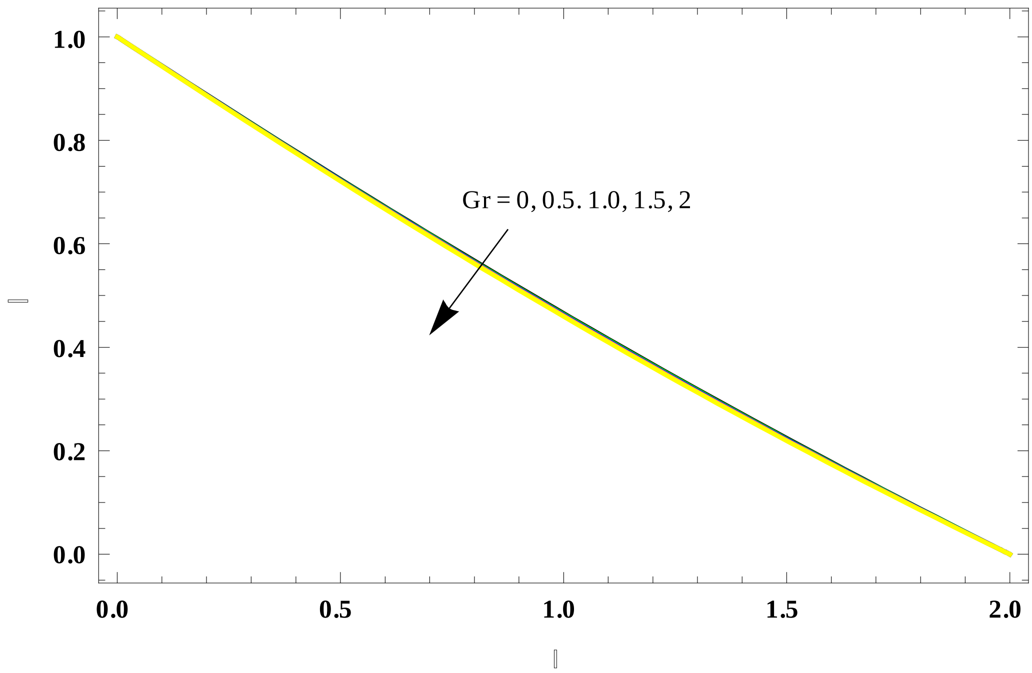

Figure 14: Impact of thermal Grashof number(Gr) on Concentration profile

Figure 14. Shows the impact of Concentration profile for different values of the Grashof number(Gr). In the figure it is observed that, for the different values of Grashof number(Gr) the concentration profile decreases with straight line.

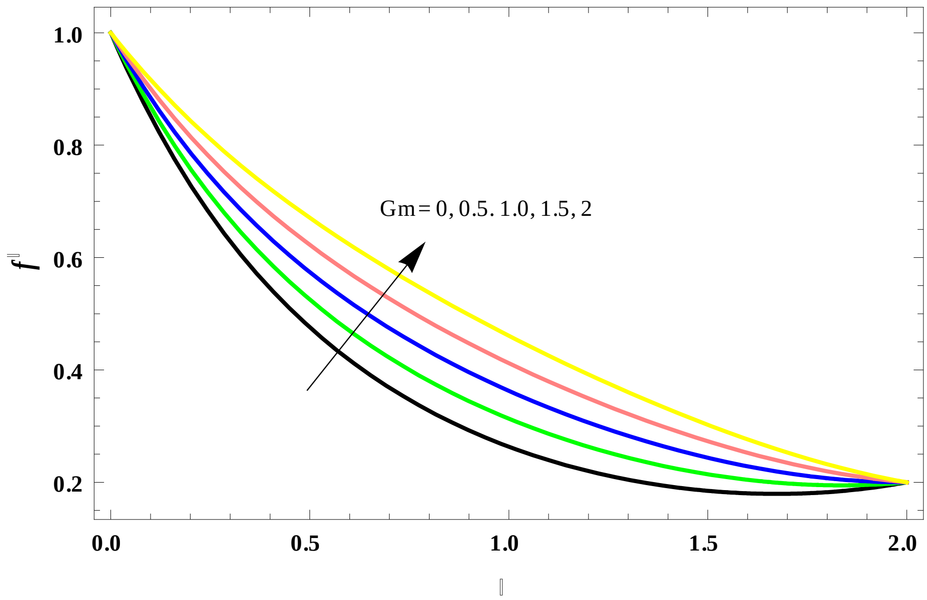

Figure 15: Impact of mass Grashof number (Gm) on Velocity

Figure 15. Demonstrates the variations in the Velocity profile for different values of the mass Grashof number (Grm). From the above figure it is seen that as the values of mass Grashof number (Grm) increases the velocity parameter decreases for different values.

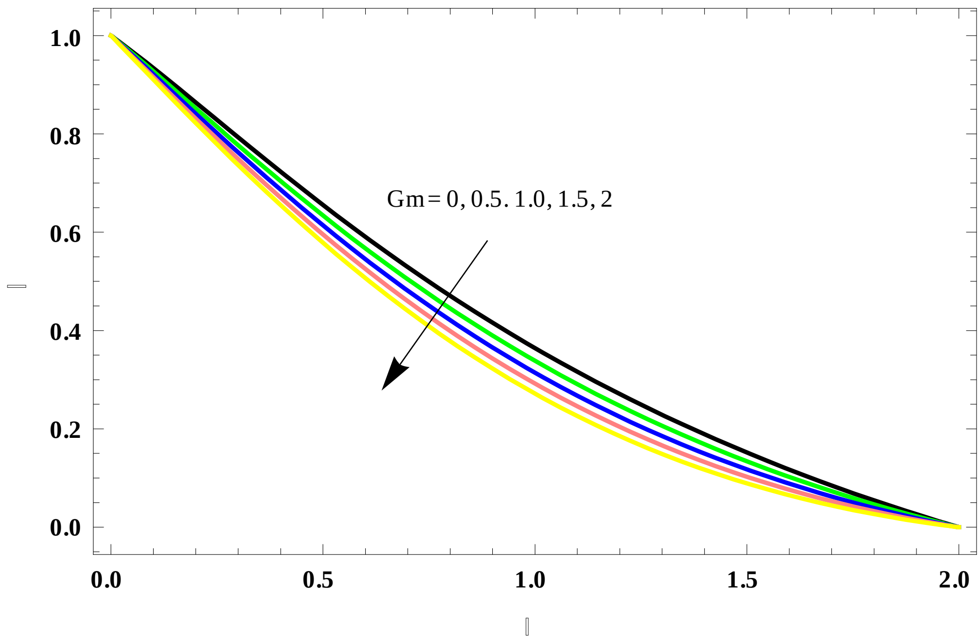

Figure 16: Impact of mass Grashof number (Gm) on temperature profile

Figure 16. Depicts the effect of temperature profile for different values of the mass Grashof number (Grm). In the figure it is seen that as the values of mass Grashof number (Grm) increases the temperature profile parameter decreases for different values.

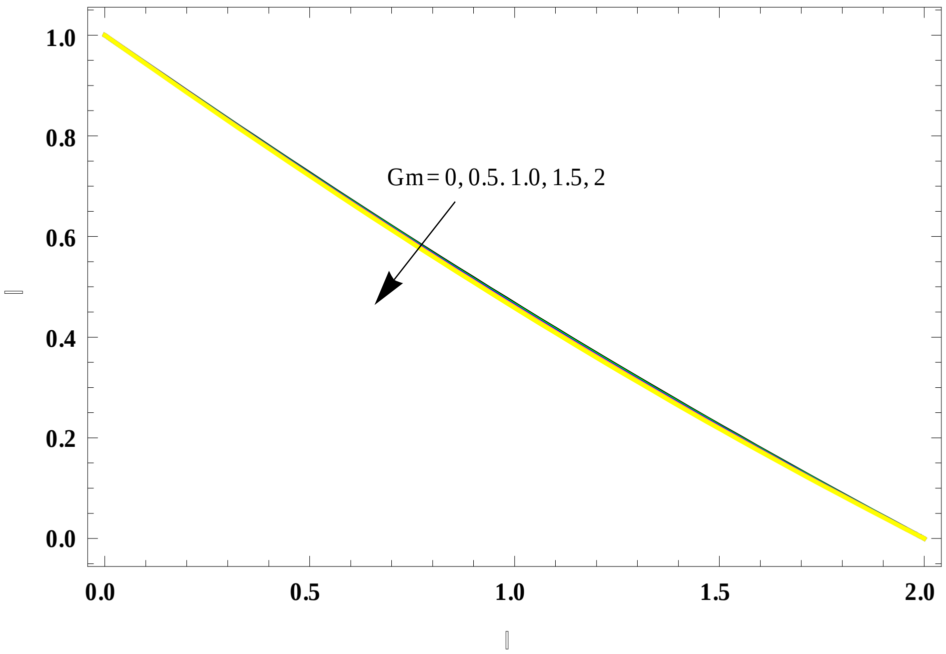

Figure 17: Impact of mass Grashof number (Gm) on Concentration profile

Figure 17. Shows the effect of Concentration profile for different values of the mass Grashof number (Grm). In the figure it is observed that, for the different values of mass Grashof number (Grm) the concentration profile decreases with straight line.

Table 1: Comparison of the values of previous works when $Pr = 1$, $Ec = 0$, $\gamma = 0$ and $\beta = 0$

λ	M. Musthafa et. Al [26]	Hashim et. Al [27]	Alfunsa Prathiba [28]	Present result
0	-	-	-1.019	-1.01201
0.1	-0.96954	- 0.96938	-0.98128	-0.98012
0.2	-0.91813	- 0.91810	-0.92627	-0.91857
0.5	-0.66735	- 0.66726	-0.67393	-0.63459
2.0	2.01767	2.017502	2.00852	2.00659
3.0	-	4.729282	-	4.547821

From table 1, it is observed that the skin friction decreases for magnetic and rotation parameter but increases for heat generation parameter. The rate of heat transfer increases for magnetic, rotation parameter and heat generation parameters and Prandtl number as an outcome the thermal boundary layer is reduced. Again, the rate of concentration increases for magnetic parameter and Schmidt number as a result the concentration boundary layer is decreased but reverse case raised for heat generation parameter.

Table 2: Comparison of the values of $f''(0)$, $\theta'(0)$ and $\phi'(0)$

λ	k	M	Pr	S	R	Ec	γ	Sc	$-f''(0)$	$-\theta'(0)$	$-\phi'(0)$
	2								1.2537	-0.0091	1.11796
0.1	10	0.5	1	0.2	0.2	0.2	0.2	0.1	1.0760	0.17105	1.12864
	100								1.0295	0.20710	1.13174
		0.5							1.2167	0.44111	1.12008
0.1	100	1	1	0.2	0.2	0.2	0.2	0.1	1.4091	0.38259	1.10981
		1.5							1.577	0.33535	1.10182
					0.3				1.4167	0.00743	0.05709
0.1	100	0.01	1	0.2	0.4	0.2	0.2	0.1	1.2165	-0.0134	1.5506
					0.5				1.2162	-0.02801	2.79238
						0.3			1.2162	-0.0124	1.57958
0.01	0.01	0.01	1	0.01	0.01	0.4	0.1	5	1.2162	-0.0602	1.63822
						0.5			1.2162	-0.1081	1.6969
							0.3		1.2162	0.0355	-0.0124
0.01	0.01	0.01	1	0.01	0.01	0.01	0.4	5	1.2162	0.0355	-0.0602
							0.5		1.2162	0.0355	-0.1081

Table 2 as the values of the porosity parameter are inflated, the skin friction values decreased and the Nusselt number, the Sherwood number enhanced. Owing to the resistance force known as the Lorentz force, the velocity and boundary thickness decreased as the magnetic field parameter was increased. The Nusselt number increases as the radiation and the Eckert number rises so that the thermal boundary layer thickness declines as it is shown in the third and fourth part of Table 2. In the fifth part of Table 2, raising the chemical reaction parameter escalated the Sherwood number that shrinks the concentration boundary layer.

5. Conclusion

This article has investigated electrically conducting MHD fluid flow of heat and mass transfer over a stretching sheet embedded in a porous medium with viscous dissipation and thermal radiation. We solved the transformed ordinary differential equations using numerical method. Effects of all controlling parameters are displayed using graphical representations and tables, the following are our findings:

- An increase in the magnetic parameter decreases the velocity profile but increases the temperature profile.
- An increase in values of thermal radiation, viscous dissipation and chemical reaction, results in the increase of velocity, temperature and heat-mass transfer rates.
- Increasing the chemical reaction parameter increases the local heat transfer rate $[-\theta'(0)]$ the Sherwood number $[-\phi'(0)]$ and the skin friction $[-f''(0)]$.

This paper plays a predominant role in science and technology applications. The results in this paper find applications in engineering such as heat exchangers, gas turbine, nuclear power plant and thermal energy storage.

References

[1] L. J. Crane, *Flow past a stretching plate*. Zeitschrift fur Angewandte Mathematik und Physik (ZAMP), 21(4), 645–647.,1970

[2] P. Carragher and L. Crane, *Heat transfer on a continuous stretching sheet*, Z. Angew. Math. Mech, vol.62, no.10, pp.564–565, 1982.

[3] A. Gupta, B. Dutta, P. Roy, *Temperature field in the flow over a stretching sheet with uniform heat flux*, Int. J Commun. Heat. MassTransf, vol.12, pp.89–94, 1985.

[4] M. Keller, Heat and mass transfer in the boundary layers on an exponentially stretching continuous surface, J. Phys. DAppl. Phys, vol.32, pp.577–585, 1999.

[5] C. Ullmann, F. Babick, and M. Stintz, *Microfiltration of submicron-sized and Nano-sized suspensions for particle size determination by dynamic light scattering*, Nanomaterials, vol.9, no.6, 2019.

[6] M. Ibrahim, Wubshet, S Bandari and M Nandeppanavar, *MHD stagnation point flow and heat transfer due to nanofluid towards a stretching sheet*, Int. J. Heat Mass Transf., vol.56, pp.1–9., 2013.

[7] M. Subhas Abel · Jagadish V. Tawade · Mahantesh M. Nandeppanavar, MHD flow and heat transfer for the upper-convected Maxwell fluid over a stretching sheet, Meccanica, 47, 385–393, 2012.

[8] M. C. K. R. and T. V. Ch. Vittal, *MHD Stagnation Point Flow and Heat Transfer of Williamson Fluid over Exponential Stretching Sheet Embedded in a Thermally Stratified Medium*, Glob. J. Pure Appl. Math., vol.13, no.6, pp.2033–2056, 2017.

[9] M. Subhas Abel, Jagadish Tawade, Mahantesh M. Nandeppanavar, *Effect of non-uniform heat source on MHD heat transfer in a liquid film over an unsteady stretching sheet*, International Journal of Non-Linear Mechanics 44, 990 – 998, 2009.

[10] Amir Abbas, Mdi Begum Jeelani, Abeer S. Alnahdi and Asifa Ilyas, *MHD Williamson Nanofluid Fluid Flow and Heat Transfer Past a Non-Linear Stretching Sheet Implanted in a Porous Medium: Effects of Heat Generation and Viscous Dissipation*, MDPI Processes 2022, 10, 1221.

[11] M. Subhas Abel, Jagadish V. Tawade, and Jyoti N. Shinde, *The Effects of MHD Flow and Heat Transfer for the UCM Fluid over a Stretching Surface in Presence of Thermal Radiation*, Hindawi Publishing Corporation Advances in Mathematical Physics, Article ID 702681, 21 pages, 2012.

[12] M. Tanyeri, M. Ranka, and C. M. Schroeder, *Microfluidic-based hydrodynamic trap: design and implementation*, Lab Chip, 11, 1786-1794, 2011.

[13] J. V. Tawade, C.N. Guled, S Noeiaghdam, U Fernandez-Gamiz, V Govindan, S Balamuralitharan, *Effects of thermophoresis and Brownian motion for thermal and chemically reacting Casson nanofluid flow over a linearly stretching sheet*, Results in Engineering, Volume 15, Article ID 100448, 2022.

[14] A. T. Brimmo and Mohammad A. Qasaimeh, RSC Advances, Stagnation point flows in analytical chemistry and life sciences, pp.51206–51232, 2017.

[15] P. Seth, G., & Mandal, *Analysis of Electromagnetohydrodynamic Stagnation Point Flow of Nanofluid Over a Nonlinear Stretching Sheet with Variable Thickness*, Journal of Mechanics vol.35, no.5, pp.719–733, 2019.

[16] M. Mustafa, T. Hayat, I. Pop, S. Asghar, and S. Obaidat, *Stagnation-point flow of a nanofluid towards a stretching sheet*, Int. J. Heat Mass Transfer. Vol.54, no. 25–26, pp.5588–5594, 2011.

[17] N. Bachok, A. Ishak, and R. Nazar, *Flow and heat transfer over an unsteady stretching sheet in a micropolar fluid with prescribed surface heat flux,* Int. J. Math. Model. Methods Appl. Sci., vol.4, no.3, pp.167–176, 2010.

[18] G. S. Roopa, B. J. Gireesha, and C. S. Bagewadi, *Numerical investigation of mixed convection boundary layer flow of a dusty fluid over an vertical surface with radiation,* Afrika Mat., vol.24, no.4, pp.487–502, 2013.

[19] P. Besthapu, R. U. Haq, S. Bandari, and Q. M. AlMdallal, *Thermal radiation and slip effects on MHD stagnation point flow of non-Newtonian nanofluid over a convective stretching surface,* Neural Comput. Appl., vol.31, no.1, pp.207–217, 2019.

[20] N. N. Reddy, V. S. Rao, B. R. Reddy, *Chemical reaction impact on MHD natural convection flow through porous medium past an exponentially stretching sheet in presence of heat source/sink and viscous dissipation,* Case Studies in Thermal Engineering, Volume 25, 100879, 2021.

[21] S. Abdal, I. Siddique, A. S. Alshomrani, F. Jarad, I. S. Ud Din, and S. Afzal, *Significance of chemical reaction with activation energy for Riga wedge flow of tangent hyperbolic nanofluid in existence of heat source,* Case Stud. Therm. Eng., vol.28, no. p.101542, 2021,

[22] R. Mohana Ramana, K. Venkateswara Raju, J. Girish Kumar, *Multiple slips and heat source effects on MHD stagnation point flow of Casson fluid over a stretching sheet in the presence of chemical reaction,* Materials Today: Proceedings, Volume 49, Part 5, Pages 2306-2315, 2022.

[23] A.Prathiba, *Stagnation Point Flow of Magnetohydrodynamic Liquid across a Linear Stretching Sheet: A Numerical Study,* International Journal of Science and Research (IJSR) 10(11):1267 – 127, 2021

[24] S.S.Benal, J.V. Tawade, M.M.Biradar, A.L.Haiter, *Effects of the Magnetohydrodynamic Flow within the Boundary Layer of a Jeffery Fluid in a Porous Medium over a Shrinking/ Stretching Sheet,* Hindawi Mathematical Problems in Engineering, Article ID 7326504, 11 pages, 2022.

[25] C. N. Guled, J. V. Tawade, Mahantesh M. Nandeppanavar, A. R. Saraf, MHD slip flow and heat transfer of UCM fluid with the effect of suction/injection due to stretching sheet: OHAM solution, Heat Transfer, 51:3201–3218, 2022.

[26] M. Mustafa, T. Hayat, I. Pop, S. Asghar, and S. Obaidat, *Stagnation-point flow of a nanofluid towards a stretching sheet.* International Journal of Heat and Mass Transfer, 54(25-26), pp.5588-5594, 2011.

[27] H. Hasmawani, M.M.Anuar, H. Abid, I. Nazila, S. Norhafizah, and S.M.Zuki, *Flow and Heat Transfer Analysis of Williamson Viscous Fluid on the Stagnation Point Past a Stretching Surface with Viscous Dissipation and Slip Conditions,* The National Conference for Postgraduate Research 2016, Universiti Malaysia Pahang, 2016.

[28] M. Ali, M.S. Alam, M.Z.U. Chowdhury, and M.A. Alim, *MHD boundary layer flow of heat and mass transfer over a stretching sheet in a rotating system with Hall current,* Journal of Scientific Research, 8(2), pp.119-128, 2016.